

1N-26

32303

103

NASA Technical Memorandum 104119

Test of Superplastically Formed Corrugated Aluminum Compression Specimens With Beaded Webs

Randall C. Davis
Dick M. Royster
Thomas T. Bales
William F. James
Joseph M. Shinn, Jr.

June 1991

(NASA-TM-104119) TEST OF SUPERPLASTICALLY
FORMED CORRUGATED ALUMINUM COMPRESSION
SPECIMENS WITH BEADED WEBS (NASA) 33 p

N91-29373

CSCC 11F

Unclass

G3/24 0032505



National Aeronautics and
Space Administration

Langley Research Center
Hampton, Virginia
23665-5225



SUMMARY

Circular cylindrical shells with corrugated wall sections provide a highly efficient structure for carrying compressive loads in aircraft and spacecraft fuselages. The superplastic forming (SPF) process offers a means to produce complex shells and panels with corrugated wall shapes. A study was made to investigate the feasibility of superplastically forming 7475-T6 aluminum sheet into a corrugated wall configuration and to demonstrate the structural integrity of the construction by testing. The corrugated configuration selected for this study has beaded web segments separating curved-cap segments. Eight test specimens were fabricated for this study. Two specimens were simply a single sheet of aluminum superplastically formed to a beaded-web, curved-cap corrugation configuration. Six specimens were single-sheet corrugations modified by adhesive bonding additional sheet material to selectively reinforce the curved-cap portion of the corrugation. The specimens were tested to failure by crippling in end compression at room temperature.

INTRODUCTION

Performance improvements for high-altitude, high-speed aircraft and spacecraft have motivated the search for minimum-mass fuselage and tank structures. Some fuselage structural concepts for such aircraft have an external heat shield that provides the aerodynamically smooth surface. In such concepts, the fuselage primary structure carries the fuselage loads and supports the heat shields, and therefore is not required to have a smooth outer surface. A corrugated wall construction can be used in this type of structural concept. An important limiting load in aircraft structure is compression buckling in the fuselage wall. A number of structural concepts designed to carry compressive loading have been investigated (ref. 1). Of the concepts, the curved-cap corrugation with beaded webs offers a very attractive mass-strength efficient wall construction for carrying compression loads. Recent advances in the state of the art of superplastic forming for aluminum materials offer a new dimension in freedom to design wall sections with this type of corrugation (refs. 2-6).

The object of the present study is to investigate the feasibility of fabricating sheet aluminum into a corrugated panel with curved caps and beaded webs by using superplastic forming and to demonstrate the structural integrity of this type of corrugation. Panel specimens superplastically formed with this unique configuration in aluminum have not previously been fabricated. Details of specimen fabrication and testing are discussed in this paper.

SPECIMEN FABRICATION

Superplastic Forming

The superplastic forming facility (fig. 1) is comprised of the stainless steel die insert, mold, cover plate, ceramic heating platens, hydraulic press, and an argon gas pressurizing system. The mold with the die tooling in place and cover plate (fig. 1(b)) is placed between the ceramic heating platens mounted in the hydraulic press. The heated platens provide the required heat source. Insulation placed along the perimeter of the mold and platens reduces heat loss. The hydraulic press applies pressure to the mold to maintain a seal between the aluminum sheet being formed and the cover plate which has a raised bead around the perimeter of the die cavity to form a seal. The press also supplies the reaction force to counter the argon gas pressure during the SPF process. The argon gas pressurizing system provides the force necessary to SPF the aluminum sheet.

A schematic of the mold and die insert is shown in figure 2. The die insert with the curved-cap, beaded-web corrugation panel shape is cast to size using 17-4 stainless steel.

The superplastic forming procedure consists of preheating the mold with the die and cover plate in place. The ram of the hydraulic press is lowered to expose the mold. A chemically cleaned 0.020-inch-thick sheet of 7475 aluminum coated with a die release compound containing boron nitride is placed on top of the mold. The ram is raised to force the sheet into contact with the cover plate. An initial load of 10,000 pounds is placed on the mold through the hydraulic press. The aluminum sheet is heated to a temperature of approximately 960°F. A seal is established as the aluminum sheet is formed around a bead on the cover plate. Superplastic forming is initiated when the aluminum sheet reaches 960°F.

The 7475 aluminum specimens were superplastically formed by one of two methods. Both methods use the same basic pressure-time profile to form the aluminum at the optimum strain rate. Each method reportedly alleviates cavitation. (Oral presentation given at the TMS Conference, Phoenix, Arizona, January 25-28, 1988, entitled "Alleviation of Cavitation in Superplastically Formed 7475 Using Post Forming Pressure," by Thomas T. Bales, Joseph M. Shinn, Jr., and William F. James.) The first method regulates the argon gas pressure on both sides of the aluminum sheet during superplastic forming phase to reduce nucleation and growth of cavities (ref. 3). This method is identified as the "back pressure" process. In the "back pressure" process, a 300 psi pressure is applied to both sides of the aluminum sheet prior to increasing the forming pressure to 385 psi (see fig. 3).

The second method regulates the argon gas pressure only on the top side of the aluminum sheet during the superplastic forming phase. A gas pressure of 85 psi forms the aluminum sheet over the die insert. At the completion of the

superplastic forming phase, a "post-forming" pressure of 300 psi is applied to the top side for a period of 60 minutes (see fig. 4) while the sheet is held at temperature. This method is identified as the "post-forming" process.

At the completion of each forming phase, the argon gas pressure is reduced to zero, the hydraulic ram is lowered, and the superplastically formed specimen removed with a special tool. The specimen is chemically cleaned and excess material trimmed away. Four specimens were superplastically formed by each of the two methods. The specimen geometry and properties are tabulated in Table I.

Specimen Construction

Specimens 1 and 2 are single sheets of aluminum just as they were SPF into corrugated sections in the mold (fig. 5). Specimens 3 and 4 are single SPF corrugation sheets with a 1.13-inch-wide reinforcing cap strip adhesive bonded to the center corrugation cap (fig. 6). The partial cap segments on the edges of these two specimens did not have an attached cap strip. Ample adhesive was used to completely wet and fill the faying surface and to produce a generous fillet along the beaded web-cap interface. Specimens 5 and 6 (fig. 7) are single-sheet corrugations with a superplastically formed 1.40-inch-wide crimped edge reinforcing cap-strip adhesive bonded to the center corrugation cap. Specimens 7 and 8 (fig. 8) are like specimens 5 and 6, except they have crimped-edge reinforcing cap-strip adhesive bonded to the partial cap segments on the edge of the specimens as well. Figure 9 shows a photograph of specimen 7 ready for test following potting of the panel ends and machining the panel ends flat, parallel and perpendicular to the axis of the curved cap.

Specimen Testing

The specimens were tested in end compression using a 1.3 MN capacity (300,000 lb.) hydraulic testing machine (see fig. 10). The edges of the specimens were supported with knife edge supports positioned 6.35 mm (0.25 inch) from the edges. Relative motion between the upper and lower heads of the testing machine was determined using three linear variable differential transformers (LVDT). The LVDT displacements were converted to strains by dividing the readings by the length of the specimen. Back-to-back foil strain gauges were bonded to the caps and were used to measure local strains. Data was recorded every 2 seconds up to two-thirds of the predicted failure load, and every second thereafter to maximum load. All of the specimens were tested at a load rate of 1500 lb./minute.

RESULTS

Specimen Compressive Stiffness

In a curved-cap, beaded-web corrugated cross section, the compressive load is carried by the caps. The beaded webs have essentially zero compressive load-carrying ability. The compressive stiffness for each specimen is the product of the load-carrying cap area and the material modulus. Computing the load-carrying cap area (the product of the cap width and thickness) is complicated by the fact that the width of the SPF cap varies along the length of the specimen. The edges of the cap have a sine-wave shape formed by the intersection of the cap with the SPF beaded web (fig. 5). The effective width of the cap is taken to be the average width between the sine-wave shaped edges. The resulting computed load-carrying areas and stiffnesses, as well as the dimensions of the specimens, are given in Table I.

The slope of the load-strain curves for a specimen is the experimental value for compressive stiffness. The load-strain response curves for the eight specimens are shown in figures 11-18. The average of the slopes of these curves gave the experimental stiffness values given in Table I. Dividing the experimental compressive stiffness by the nominal material modulus of $10.2 E_6$ psi gives the values for experimental load-carrying area for the cross section. These results are also given in Table I.

The computed total weight of the specimens is found using the initial 0.02-inch thickness of the sheet material before it is superplastically formed. Thus, the weight of the SPF portion of the specimen shown in Table II is the product of the specimen width, length, the 0.02-inch initial thickness, and the material density. The weight of the additional cap material bonded to specimens 3 through 8 shown in Table II is computed from the cap geometry and is added to the SPF segment weight to give the computed total weight values shown in Table II. Each specimen was weighed and these measured total weights are shown in Table II for comparison with the computed total weights. The agreement is excellent.

The computed total weight for the specimen minus the product of the computed load-carrying area, the specimen length, and density gives the computed weight of material in the beaded-web portion of the specimens. These results, divided by specimen length, give the computed beaded-web weight per unit length values shown in Table II. The measured total weight for the specimens divided by the panel length are also shown in Table II for comparison. The slightly higher measured weight values for specimens 7 and 8 are attributed to the weight of the adhesive bonding used to bond the additional cap material in place.

The experimental and calculated weight and load-carrying area values given in Tables I and II show excellent agreement. This gives confidence in the accuracy of the geometric dimensions and material properties used for the test specimens and used to construct analytical models of the specimens. These models were developed for use in the PASCO analysis code (ref. 7) to compute buckling loads for the specimens.

Panel Tests

The load-strain test results, shown in figures 11-18, are nondimensionalized by dividing the test loads by the product of the material yield strength times the specimen computed load-carrying area, and by dividing the test strains by the yield strength divided by material modulus. Thus, the theoretical slope of such normalized load-strain results lies along the diagonal from the origin of the graph and passes through the point (1,1) on the graph. The trace of the normalized test results should fall along this diagonal. Deviation of the test results above or below this diagonal indicates a discrepancy between the experimental and computed compressive stiffnesses for the specimen.

Local buckles that develop in the specimen due to applied compressive load are manifested by through-the-thickness bending in the caps. Back-to-back strain gauges located on a buckle will reveal the load at which bending becomes the dominant strain mechanism. This is noted as a divergence of the back-to-back strain gage response curves with increasing load. As a local buckle mode develops, the bending strain will increase, causing one gauge response curve to show a disproportionate increase in compressive strain with load and the other a disproportionate decrease in strain. The point, where the latter strain gauge response reaches a maximum strain value and begins to decrease with load, is used to define the reversal strain for the specimen. The load corresponding to this strain reversal point is defined as the reversal buckling load for the local buckle. The lowest load found among all the strain gauge pairs on a specimen defines the experimental reversal buckling load for the specimen given in Table III.

The overall shortening of the specimen from the applied compressive load is measured by means of differential current-displacement transducers (DCDT). The DCDT's are mounted between the platens of the test machine to detect movement of the platen heads relative to each other. The DCDT displacements are converted to strains by dividing their readings by the length of the specimen. The slope of these strain curves is the experimental compressive stiffness of the specimen. Buckles in the specimen, at high strain levels, cause a decrease in the slope of the DCDT load-strain curves (figs. 11-18).

Models of the specimens were analyzed using the PASCO code (ref. 7). The computed load-carrying areas and computed compressive stiffnesses used in the PASCO models are given in Table I. The beaded webs in the specimens are treated in a two-step modeling process in PASCO. First, a cross section through the beaded web perpendicular to the beads is modeled separately on PASCO and the results analyzed to determine the extensional stiffnesses and bending stiffnesses of the beaded web. These stiffnesses of the beaded web are used to find a three-layer equivalent laminate representation of the beaded web by the technique described in reference 1. The three-layer equivalent laminate so determined is used in place of the beaded web in the PASCO model of the specimen. PASCO analyzes the modified model to determine the buckling loads of the specimens. The computed panel buckling strains and buckling

loads from the PASCO results are shown in Table III. The results are compared with the corresponding experimentally determined results.

The first two specimens (1 and 2) failed prematurely. The SPF beaded webs create localized indentations in the caps at their junction with the beaded webs. At each of these indentations, local strain concentrations caused the cap material to begin to wrinkle early in the test. These localized deflections grew as the load was increased and eventually caused failure across the caps by local buckling. These indentations are not included in the PASCO analysis, hence the large discrepancy between the PASCO results and test. The presence of the adhesively bonded cap strips in specimens 3 through 8 prevented these local buckles from developing. The addition of an adhesive-bonded cap strip to the corrugation in specimens 3 and 4 raised the average reversal strain by 400 percent over specimens 1 and 2. The buckling strains predicted by PASCO are higher than the proportional limit strain for the material, hence the test strains are less than the analytical strains. The crimped edge added to the cap strips bonded to specimens 5 and 6 further stabilized the edge of the caps against buckling. The crimped edges increased the compressive stiffness by 20 percent, but raised the buckling reversal strain by 35 percent.

Specimens 7 and 8 did not buckle elastically like specimens 1 through 6. The crimped edges added to the cap strips of these two specimens sufficiently stabilized the caps against buckling to raise the experimental buckling strains in the caps above the proportional limit strain for the material. Strain gauge response data from specimen 7 shows a strain reversal just prior to reaching yield (point (1,1) on the non-dimensionalized plots). Strain gauge response curves from specimen 8 do not show a reversal as the cap material begins to strain beyond yield (beyond point (1,1) on the nondimensionalized plots). Therefore, Table III shows a reversal strain for panel 7 but a "---" (not applicable) for specimen 8.

Specimen Processing

Eight 7475 aluminum alloy specimens were successfully fabricated by SPF using either the "back pressure" method or "post forming" method. The time-pressure profiles were easier to control using the "back pressure" process and tighter tolerances were achieved using the "post forming" process. Figure 19 shows photo-micrographs of polished sections taken from the 7475 aluminum specimens following SPF. The microstructure from specimens using "post forming" (b) and "back pressure" (c) is compared to a specimen SPF with no pressurizing procedure to alleviate cavitation in the material (a). The decrease presence of cavitation in the SPF 7475 specimens using either "post forming" or "back pressure" is evident when compared to SPF 7475 specimens with no cavitation alleviation procedure. The load data for these specimen tests (see Table III) indicates that both processes resulted in specimens with equal load-carrying capabilities.

CONCLUDING REMARKS

The objective of this study was met. The feasibility of superplastically forming 7475 aluminum corrugated specimens with beaded webs was investigated. The structural integrity of the new concept was demonstrated by testing the specimens thus formed in end compression to failure. The junction of the corrugation cap with the beaded web causes local wrinkling in the caps that causes the caps to buckle at low strain levels. Adhesively bonding an additional reinforcing cap strip to the corrugation cap prevents these local wrinkles from growing into buckles with increasing load, thereby raising the buckling strain level by 400 percent. The addition of crimped edges to the adhesively bonded cap strips improves the buckling strain level by 35 percent over reinforcing cap strips with no crimped edges. The experimental results demonstrated the feasibility of superplastically forming aluminum corrugation with beaded webs. Local buckles precipitated by indentations in the edges of the caps were not included in the analysis, causing poor agreement between test and analysis for the specimen with no reinforced caps. Analysis showed local buckling strains in the specimens with reinforcing caps greater than the proportional limit for the material, causing the analytical buckling loads to be higher than the experimental buckling loads.

REFERENCES

1. Davis, Randall C.; Mills, Charles T.; Prabhakaran, R.; and Jackson, L. Robert: **Structural Efficiency Studies of Corrugated Compression Panels With Curved Caps and Beaded Webs.** NASA TP 2272, 1984.
2. Bales, Thomas T.: **SPF/DB Titanium Technology.** NASA CP 2160, October 1980.
3. Bampton, C. C.; and Raj, R.: **Influence of Hydrostatic Pressure and Multiaxial Straining on Cavitation in Supersplastic Aluminum Alloy.** Acta Metallurgica, Volume 30, 1982, pp. 2043-2053.
4. Royster, Dick M.; Bales, Thomas T.; and Wiant, H. Ross: **Superplastic Forming/Weld-Brazing of Titanium Skin-Stiffened Compression Panels.** Materials Overview for 1982. Volume 27 of National SAMPE Symposium and Exhibition, Society of Advanced Materials and Process Engineering, 1982, pp. 569-582.
5. Royster, Dick M.; and Bales, Thomas T.: **Elevated Temperature Behavior of Superplastically Formed/Weld-Brazed Titanium Compression Panels Having Advanced Shaped Stiffeners.** NASA TP 2123, 1983.
6. Royster, Dick M.; Bales, Thomas T.; Davis, Randall C.; and Wiant, H. Ross: **Fabrication and Evaluation of Cold-Formed/Weld Brazed Beta-Titanium Skin-Stiffened Compression Panels.** NASA TP 2201, 1983.
7. Anderson, Melvin S.; and Stroud, W. Jefferson: **A General Panel Sizing Computer Code and Its Application to Composite Structural Panels.** AIAA Journal, Volume 17, Number 8, August 1979, pp. 892-897.

Table 1 - Specimen geometry and stiffness properties

| Specimen | Center cap | | Edge caps | | Cap strip adhesive bonded to center cap | | Cap strip adhesive bonded to edge caps | | Cap strip crimped edge | | Computed load carrying area A (in. ²) | Computed compressive stiffness (lbs) | Experimental compressive stiffness (lbs) | Experimental load carrying area (in. ²) |
|----------|-------------|--------------|-------------|--------------|---|--------------|--|--------------|------------------------|--------------|---|--------------------------------------|--|---|
| | Width (in.) | Thick. (in.) | Width (in.) | Thick. (in.) | Width (in.) | Thick. (in.) | Width (in.) | Thick. (in.) | Width (in.) | Thick. (in.) | | | | |
| 1 * | 1.30 | .02 | 1.00 | .018 | none | none | none | none | none | none | .0620 | .657E6 | .657E6 | .0620 |
| 2 ** | 1.30 | .02 | 1.00 | .018 | none | none | none | none | none | none | .0620 | .657E6 | .635E6 | .0599 |
| 3 ** | 1.30 | .02 | 1.00 | .018 | 1.13 | .02 | none | none | none | none | .0846 | .897E6 | .842E6 | .0794 |
| 4 * | 1.30 | .02 | 1.00 | .018 | 1.13 | .02 | none | none | none | none | .0846 | .897E6 | .827E6 | .0780 |
| 5 * | 1.30 | .02 | 1.00 | .018 | 1.40 | .02 | none | none | .25 | .02 | .1000 | 1.060E6 | 1.000E6 | .0943 |
| 6 ** | 1.30 | .02 | 1.00 | .018 | 1.40 | .02 | none | none | .25 | .02 | .1000 | 1.060E6 | 1.003E6 | .0946 |
| 7 ** | 1.30 | .02 | 1.15 | .018 | 1.40 | .02 | 1.15 | .02 | .25 | .02 | .1610 | 1.711E6 | 1.749E6 | .1650 |
| 8 * | 1.30 | .02 | 1.15 | .018 | 1.40 | .02 | 1.15 | .02 | .25 | .02 | .1610 | 1.711E6 | 1.823E6 | .1720 |

Material modulus E = 10.6E6 psi
 Poisson ratio = .33
 Material density = .097 lb/in.³
 Proportional limit strain = .0050
 Yield stress σ_y = 65,000 psi

* = Back pressure process

** = Post forming process

Table 2 - Computed and actual specimen weights

| Specimen | Specimen | | SPF segment weight (lbs) | Added material weight (lbs) | Computed total weight (lbs) | Measured total weight (lbs) | Computed beaded web weight per length (lbs/in.) | Experimental beaded web weight per length (lbs/in.) |
|----------|-------------|----------------|--------------------------|-----------------------------|-----------------------------|-----------------------------|---|---|
| | Width (in.) | Length L (in.) | | | | | | |
| 1 | 4.72 | 7.47 | .069 | none | .071 | .069 | .0032 | .0030 |
| 2 | 4.65 | 7.49 | .070 | none | .071 | .070 | .0032 | .0033 |
| 3 | 4.74 | 5.75 | .055 | .013 | .068 | .067 | .0033 | .0036 |
| 4 | 4.75 | 5.15 | .049 | .012 | .061 | .057 | .0033 | .0032 |
| 5 | 4.65 | 5.70 | .054 | .022 | .075 | .075 | .0031 | .0036 |
| 6 | 4.64 | 5.84 | .055 | .022 | .077 | .075 | .0031 | .0033 |
| 7 | 4.78 | 7.47 | .072 | .071 | .143 | .165 | .0029 | .0054 |
| 8 | 4.84 | 7.48 | .073 | .071 | .144 | .166 | .0030 | .0048 |

Table 3 - Specimen buckling strains and loads

| Specimen | Experimental reversal strain | Experimental reversal buckling load (lbs) | PASCO buckling strain | PASCO buckling load (lbs) |
|-----------------|-------------------------------------|--|------------------------------|----------------------------------|
| 1 | .00074 | 826 | .00508 | 3339 |
| 2 | .00129 | 977 | .00508 | 3339 |
| 3 | .00430 | 3506 | .00636 | 5702 |
| 4 | .00383 | 3312 | .00636 | 5702 |
| 5 | .00514 | 4810 | .00654 | 6928 |
| 6 | .00586 | 4745 | .00654 | 6928 |
| 7 | .00408 | 8556 | .00539 | 8685 |
| 8 | — | — | .00539 | 8685 |

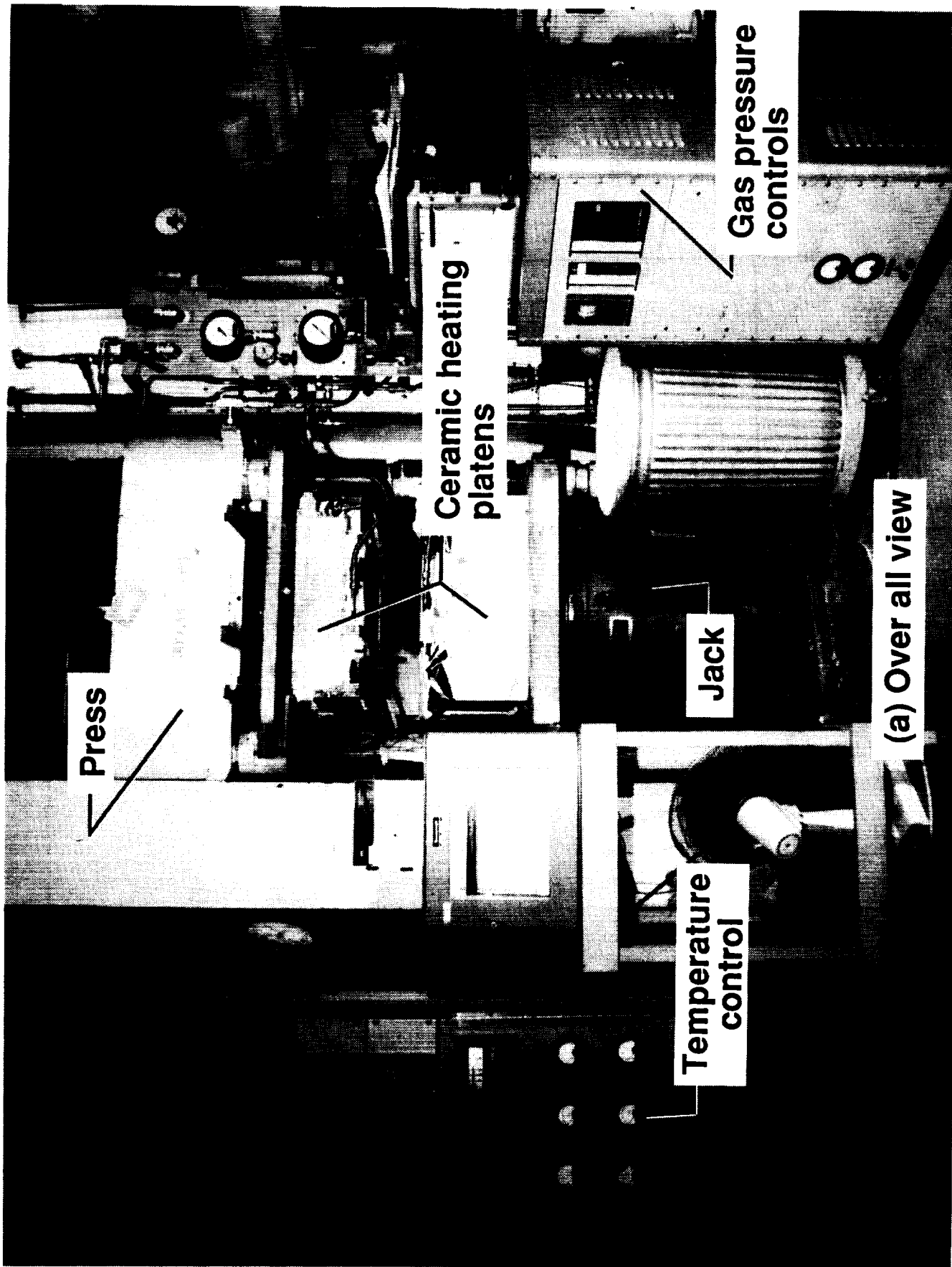
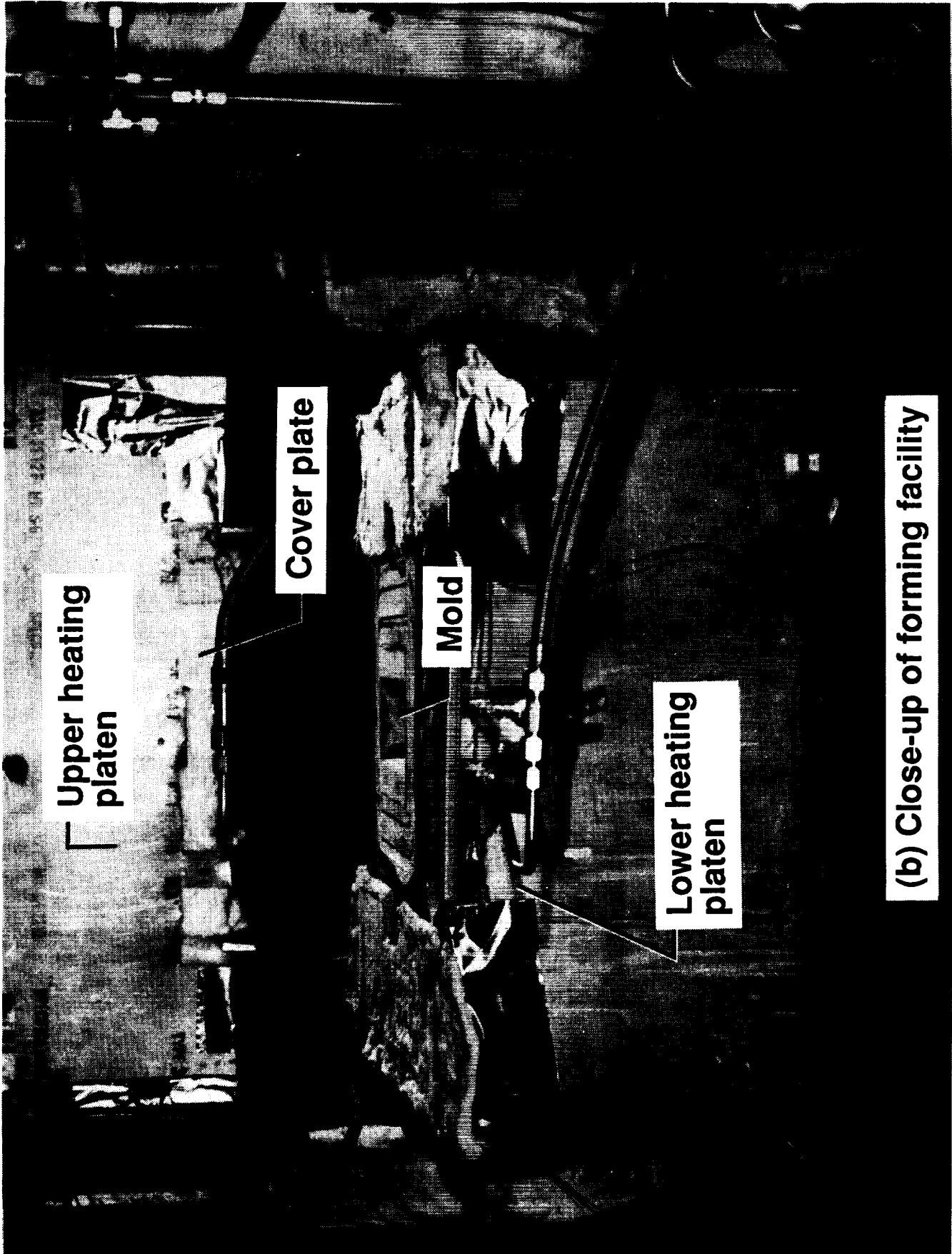


Figure 1-Superplastic forming facility



(b) Close-up of forming facility

Figure 1-Concluded

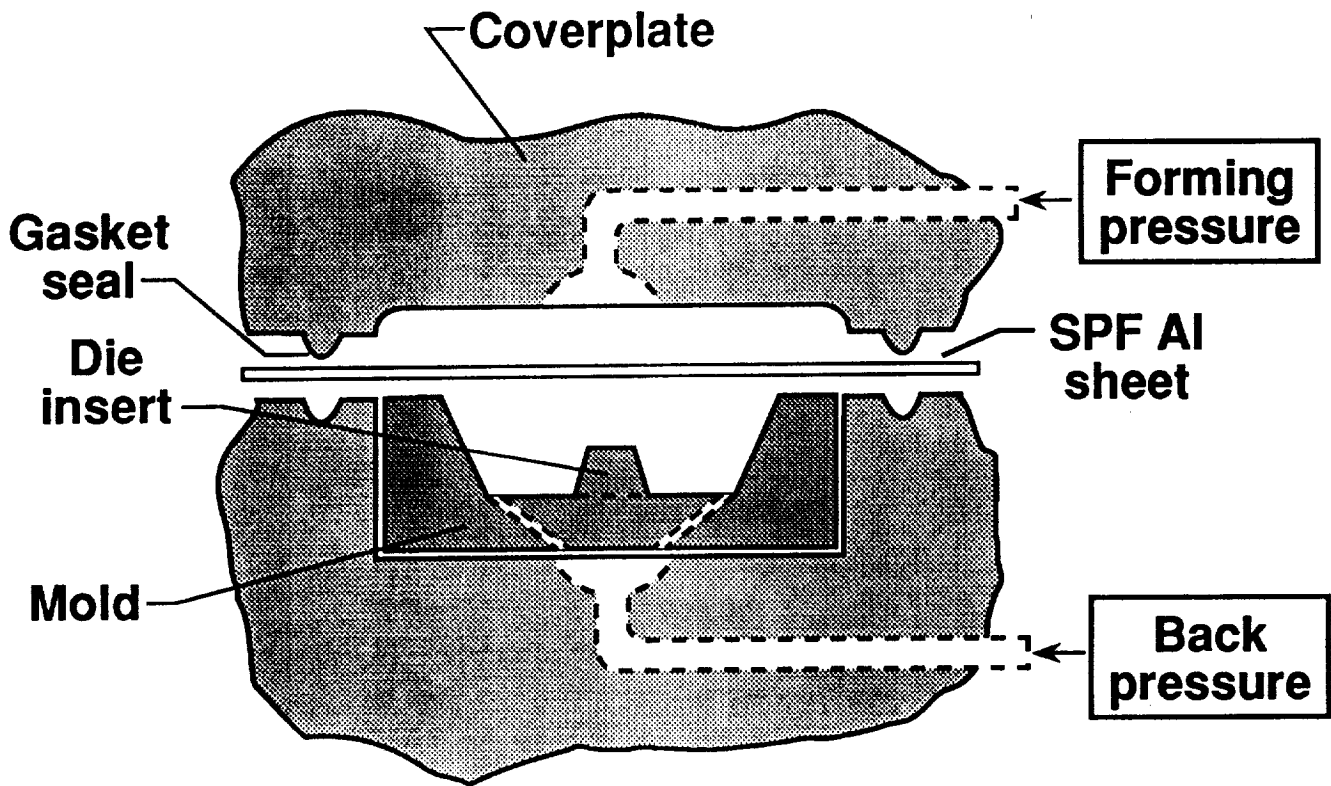


Figure 2 - Schematic of mold, cover plate and die insert

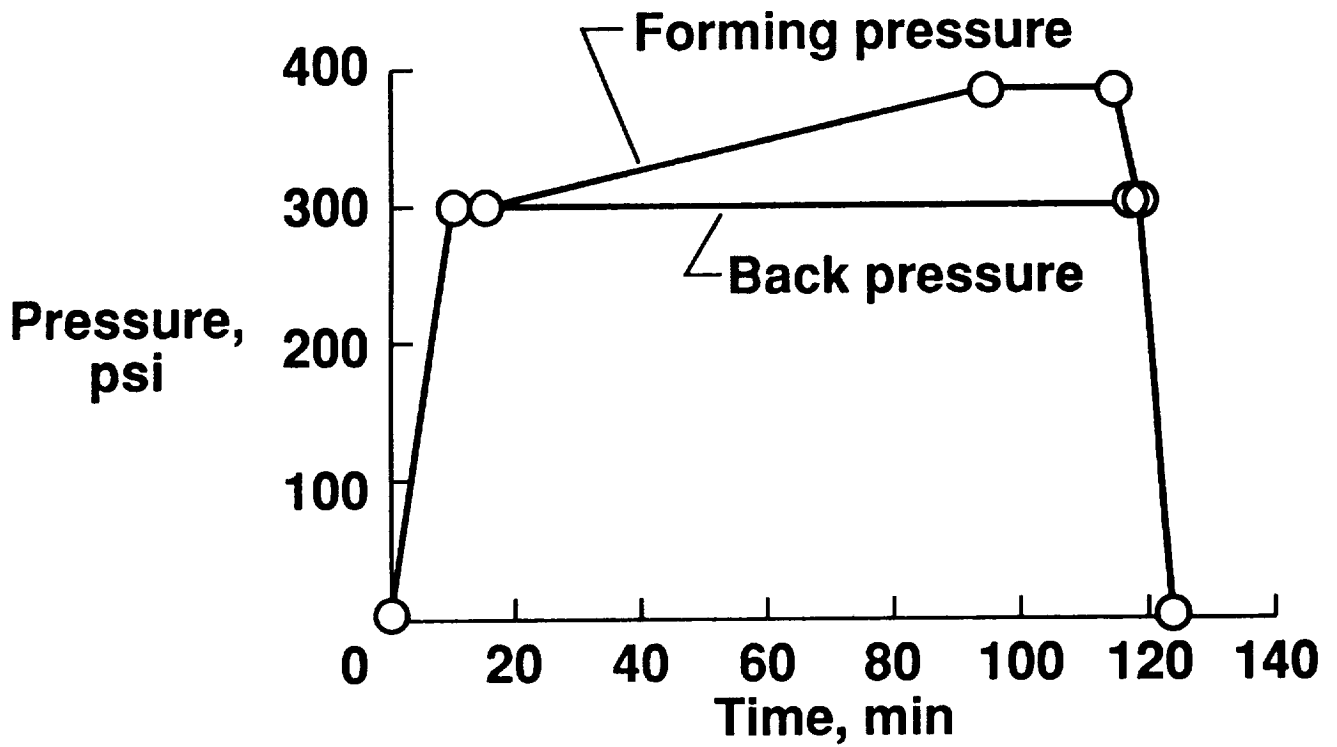


Figure 3 - Pressure - time profile used to form specimens by "back pressure" process

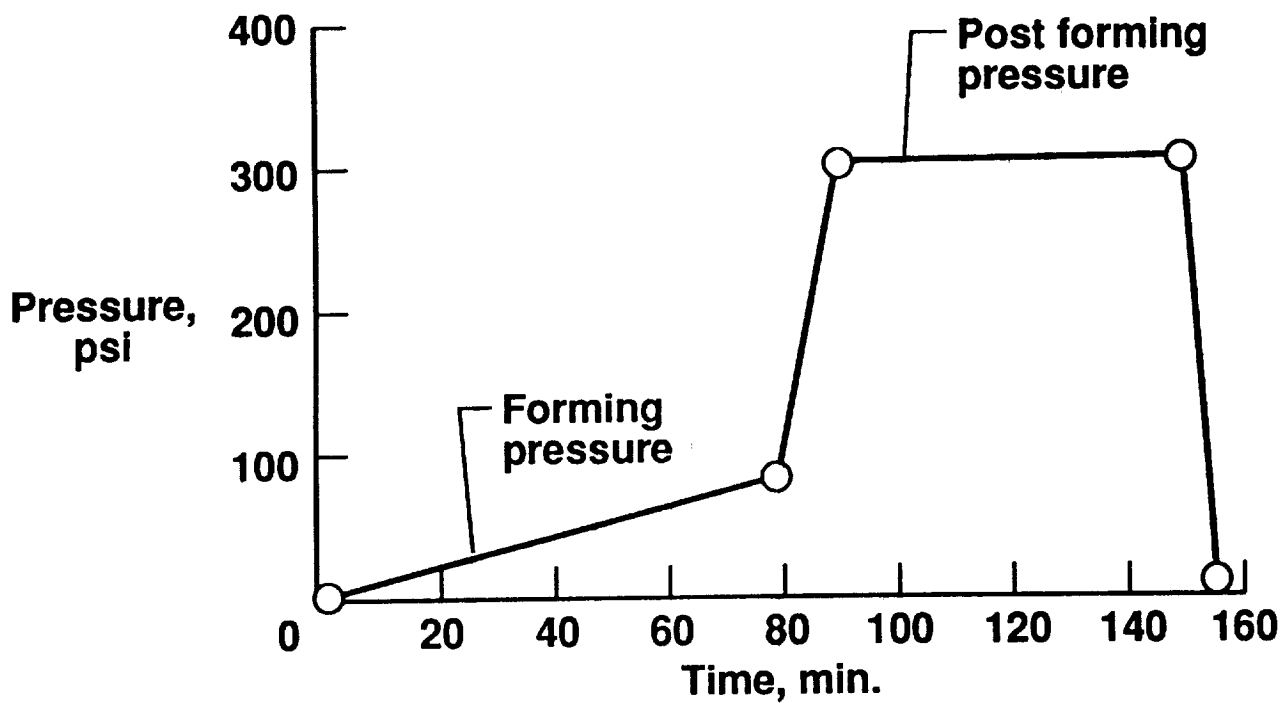


Figure 4- Pressure-time profile for forming specimens by the "post-forming" process.

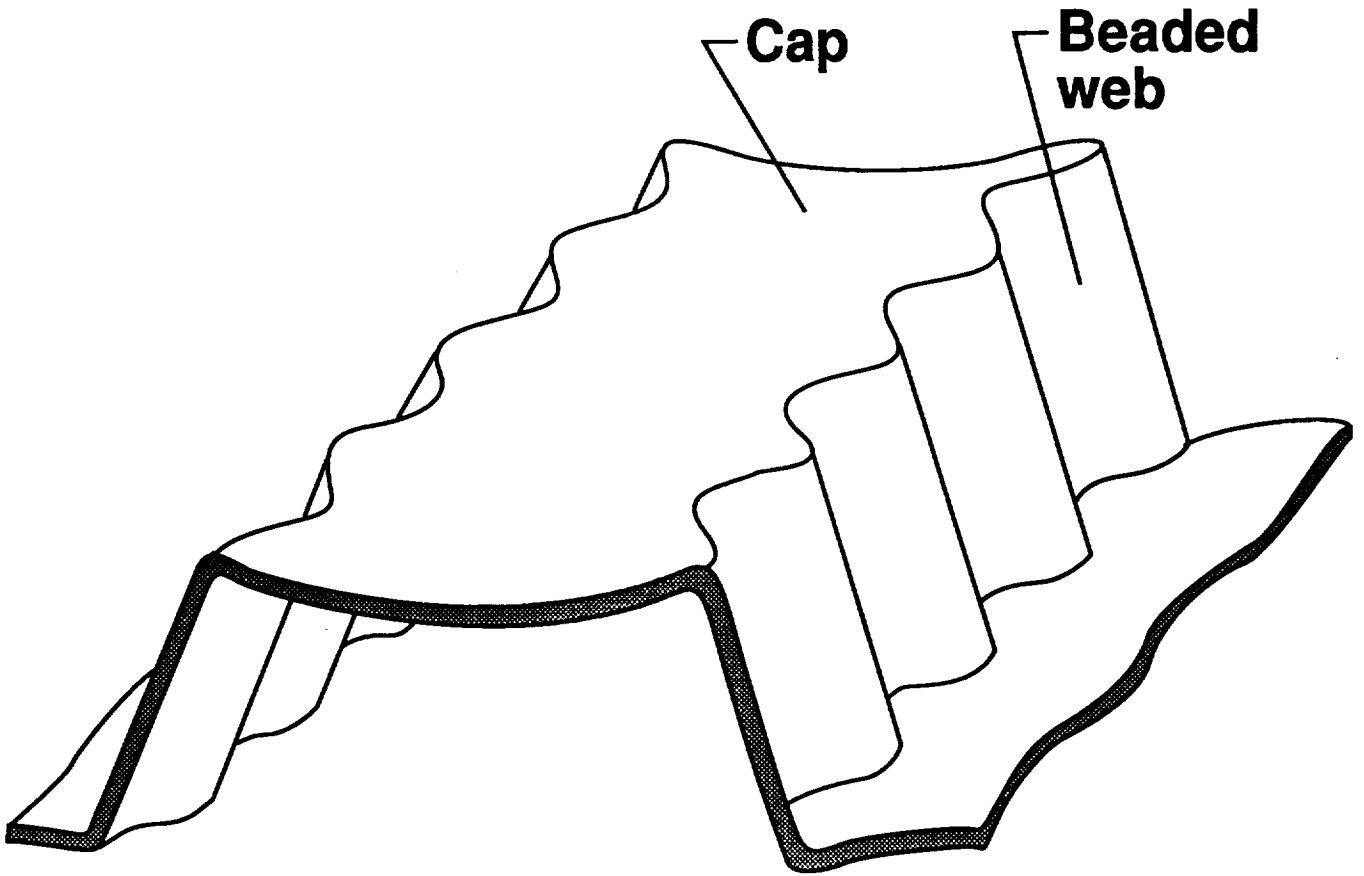


Figure 5 - Schematic of single SPF corrugated sheet construction of specimens 1 and 2

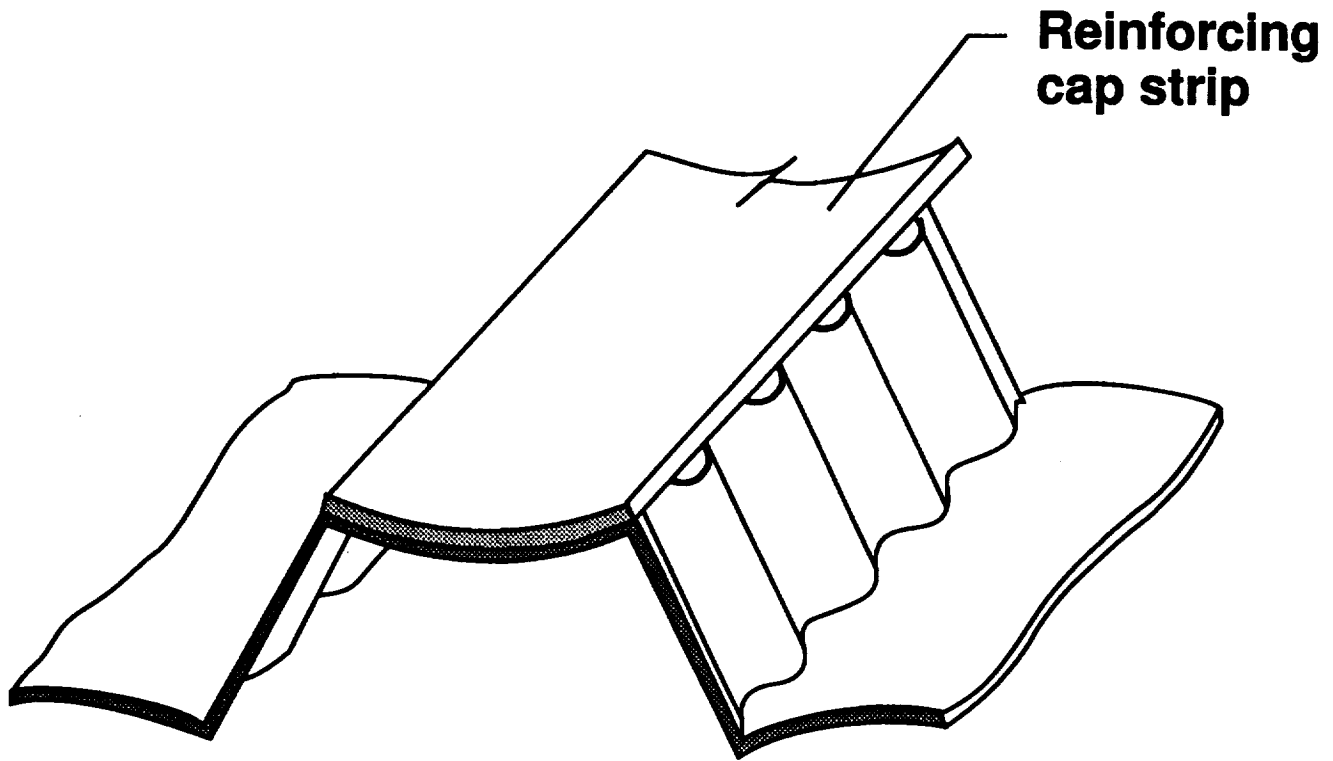


Figure 6. Schematic of specimens 3 and 4 showing cap strip brazed to center cap of the SPF corrugated sheet.

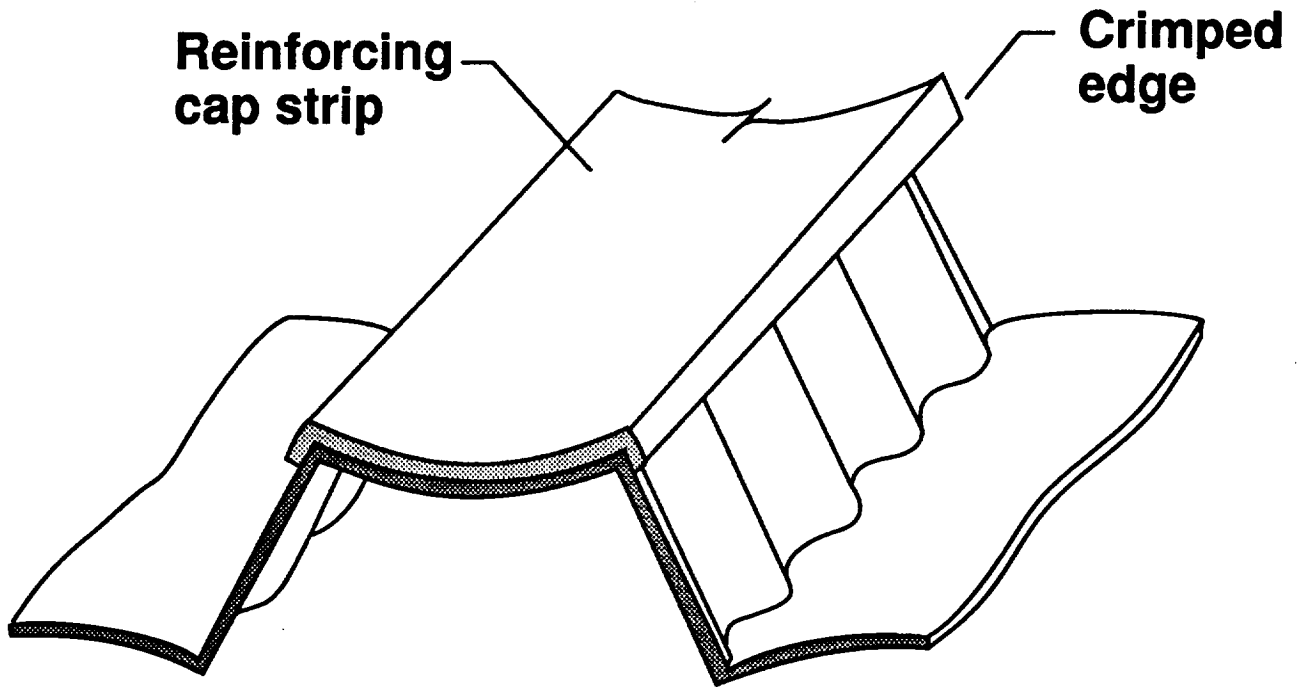


Figure 7 - Schematic of specimens 5 and 6 with cap strip with crimped edges adhesive bonded to center cap of the SPF corrugated sheet.

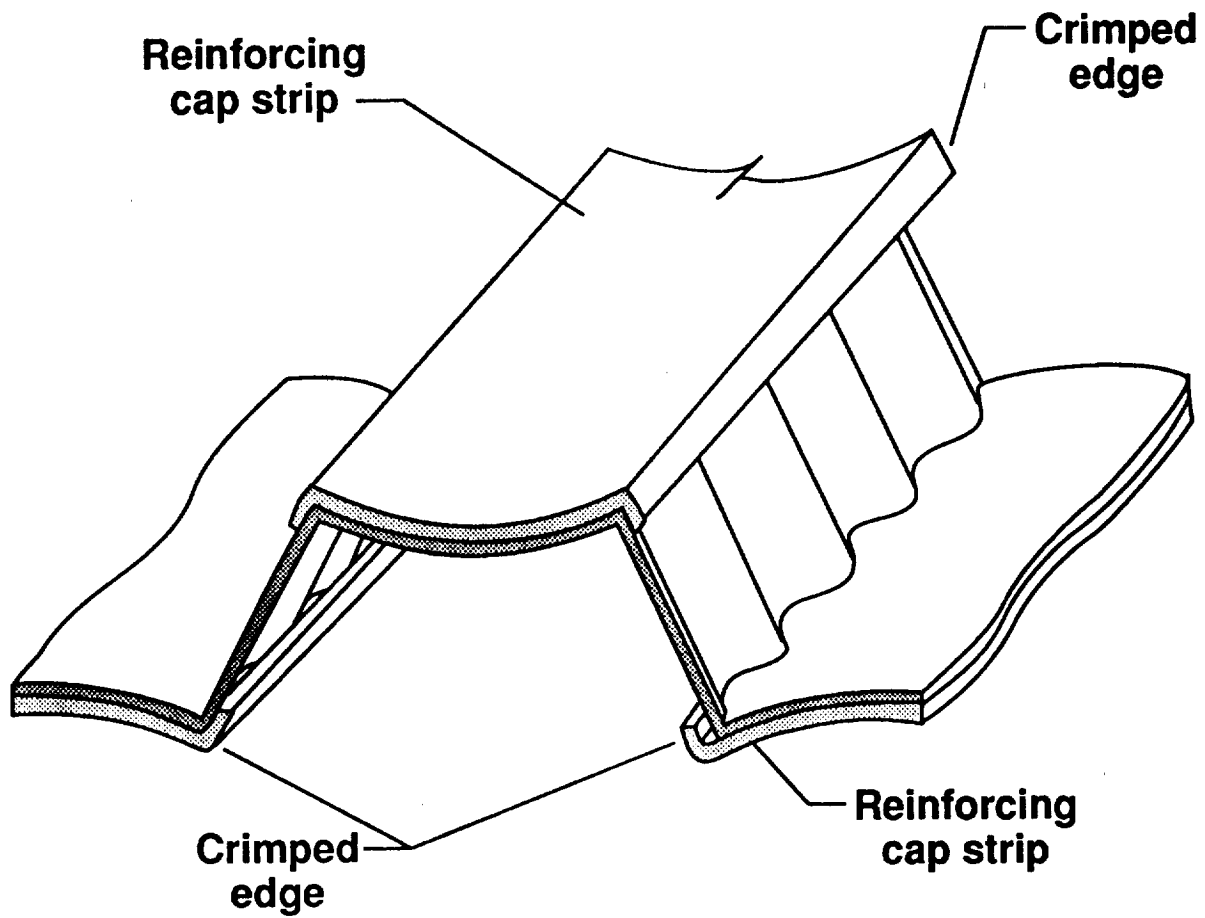


Figure 8 - Schematic of specimens 7 and 8 with cap strip with crimped edges adhesive bonded to all three caps of the SPF corrugated sheet.

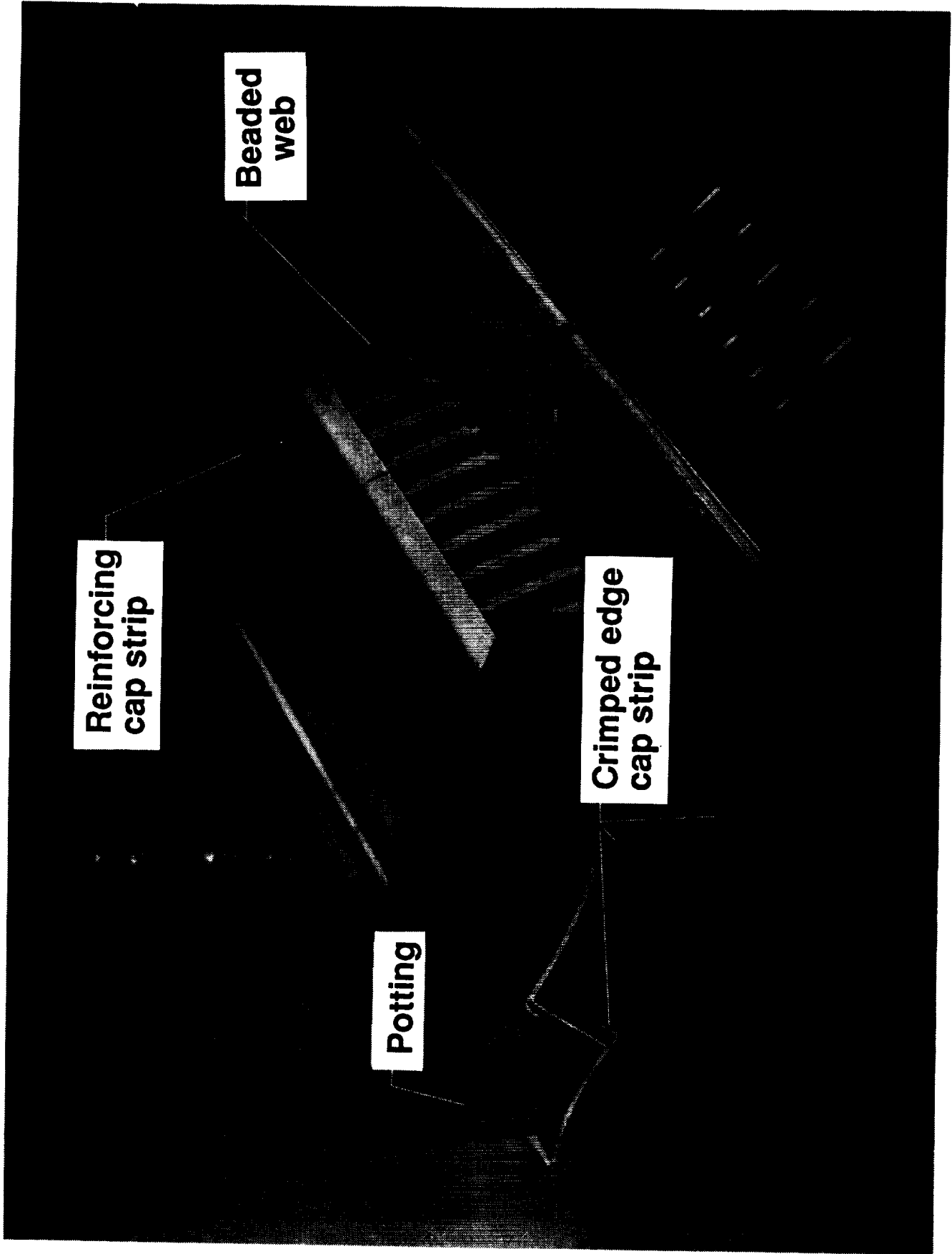
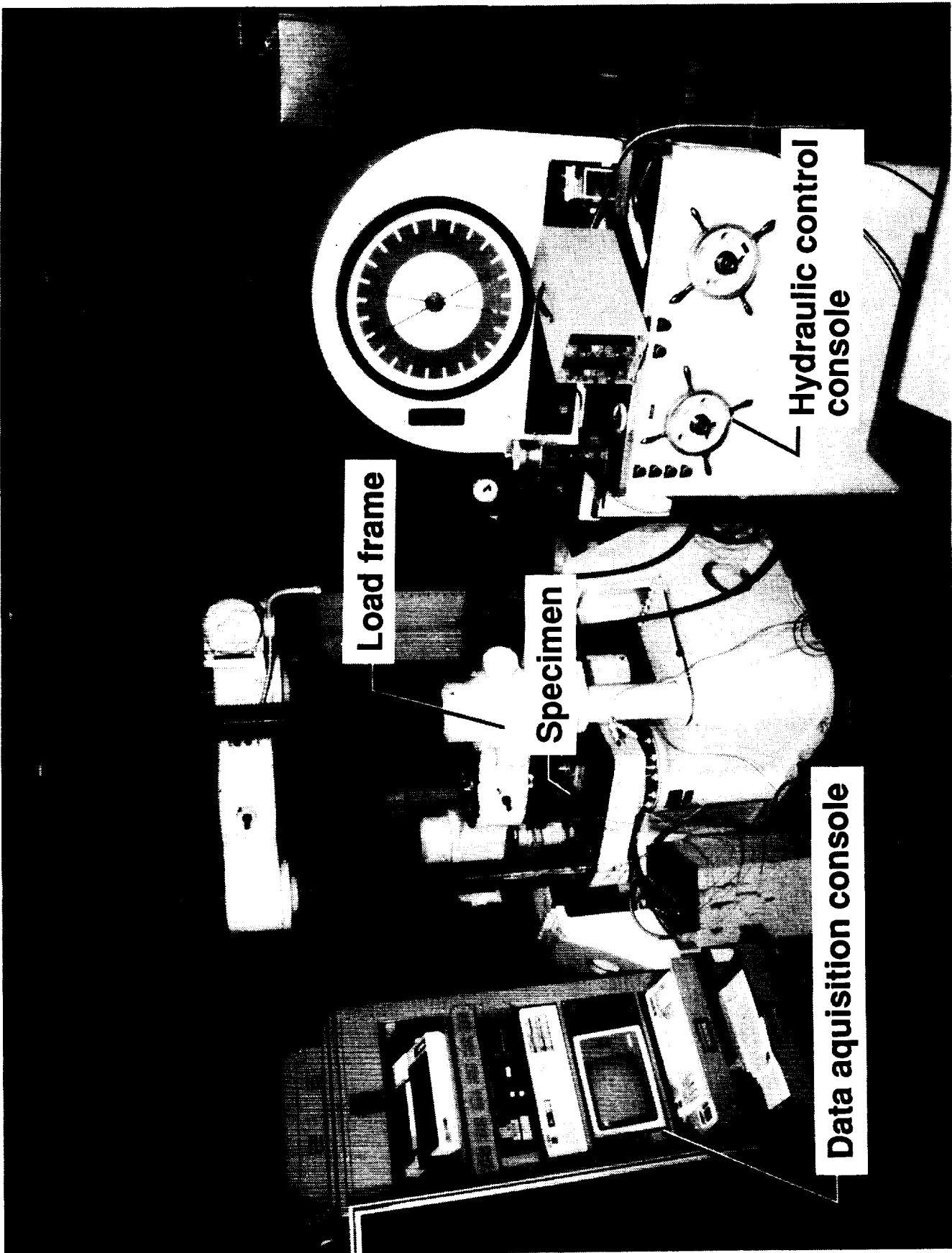


Figure 9-Single-corrugation compression specimen.
(Dimensions are in inches)



**Figure 10-Test setup for single
corrugation specimens**

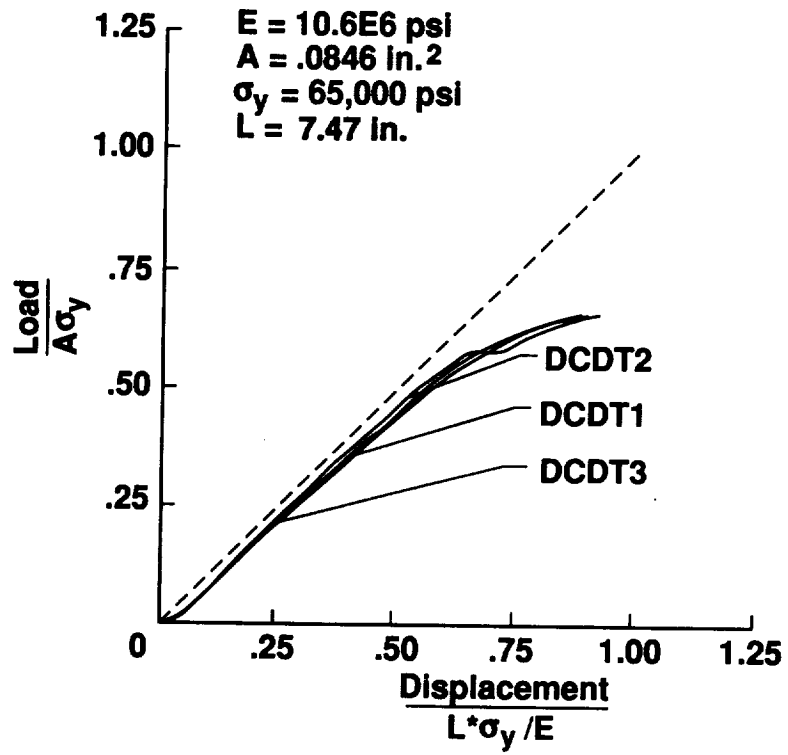
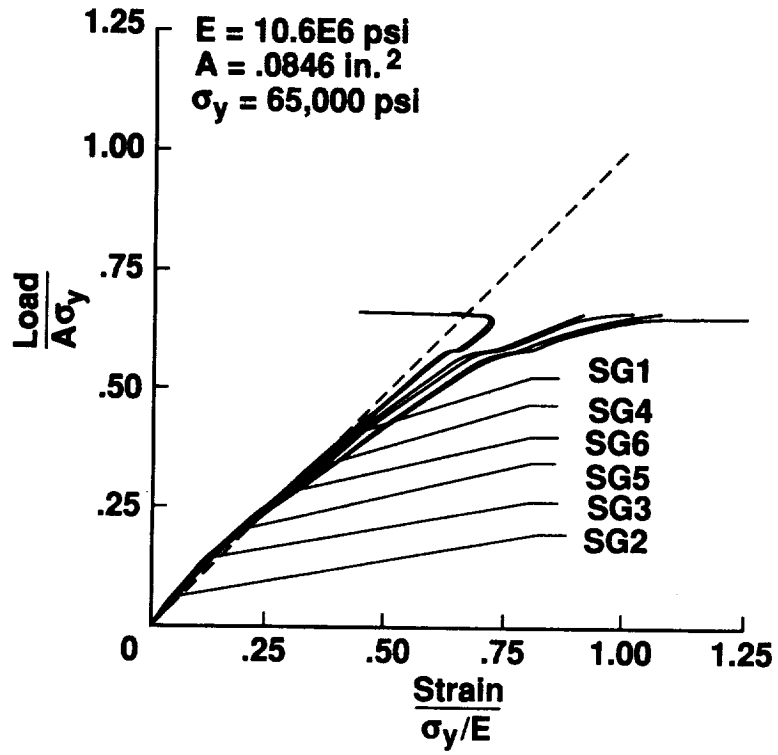


Figure 11-Strains for specimen 1

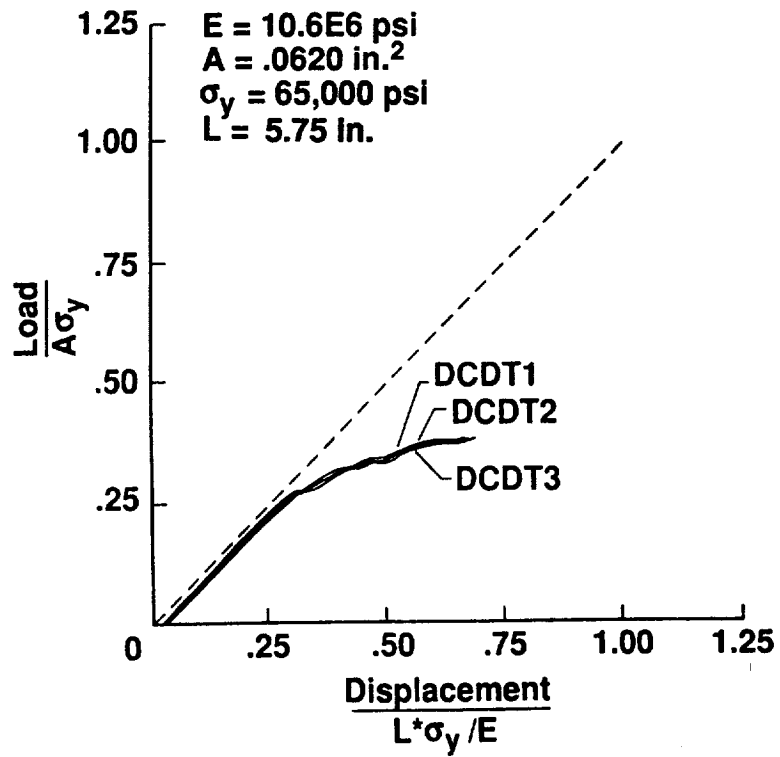
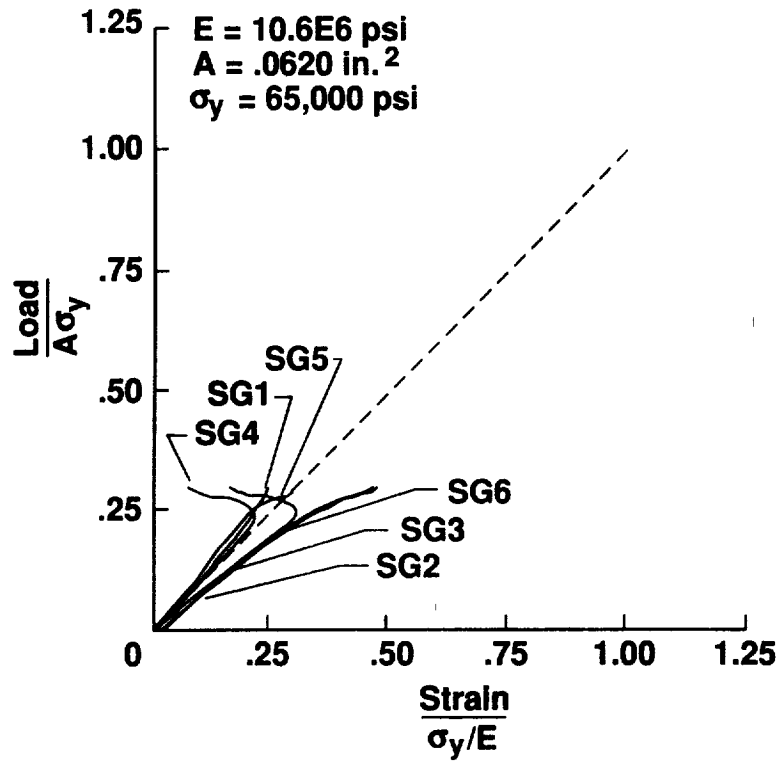


Figure 12-Strains for specimen 2

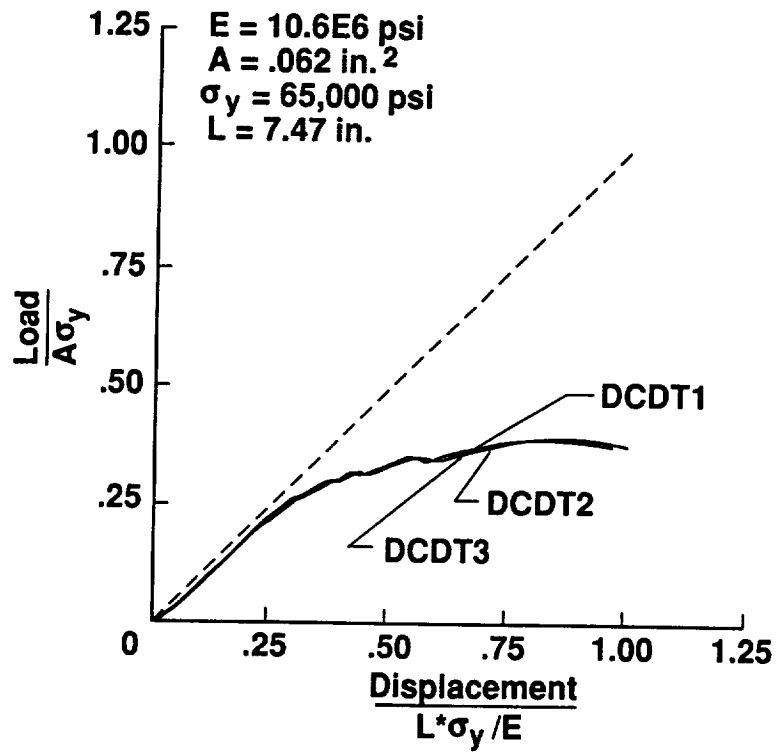
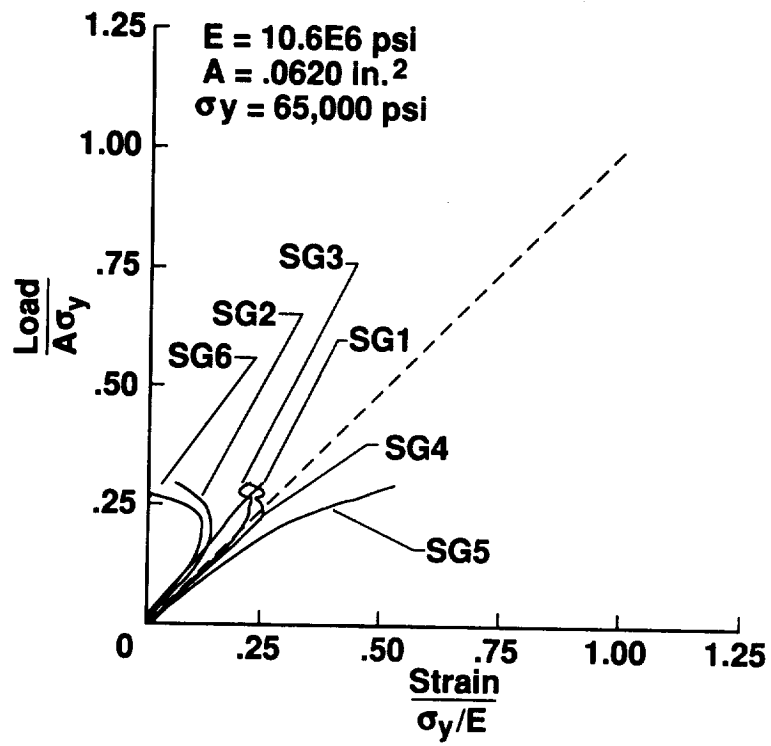


Figure 13-Strains for specimen 3

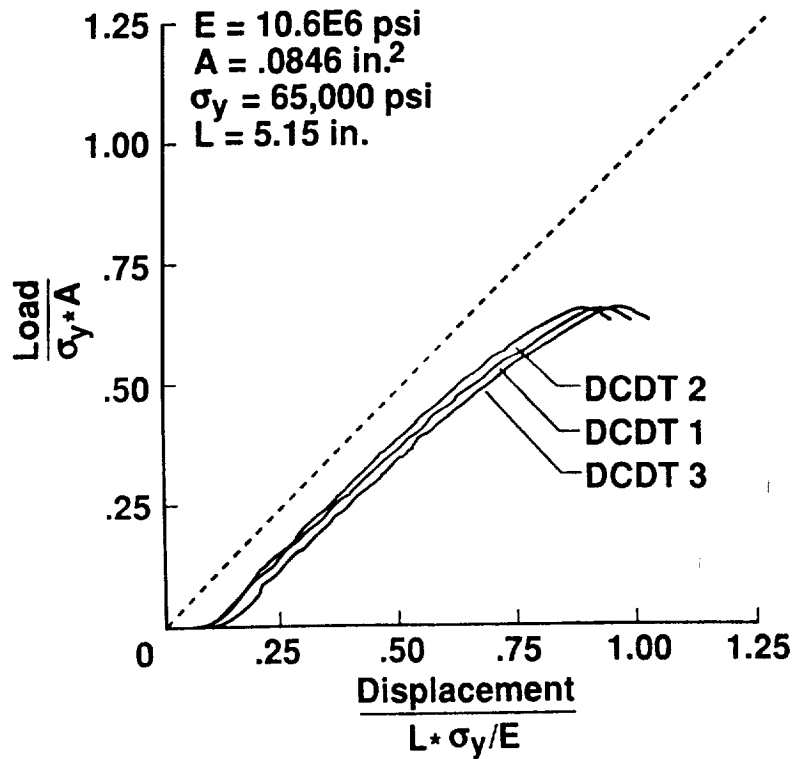
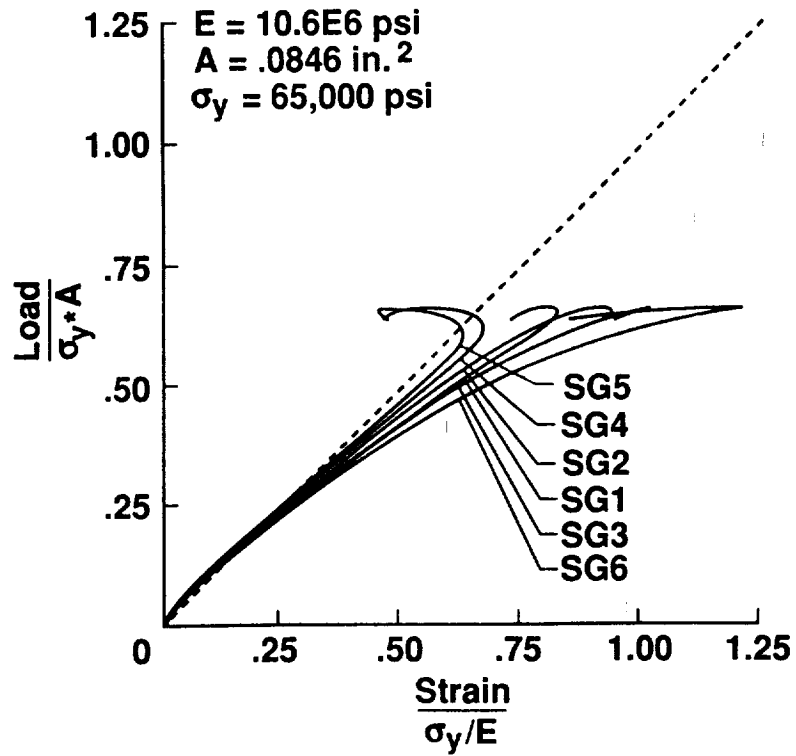


Figure 14-Strains for specimen 4

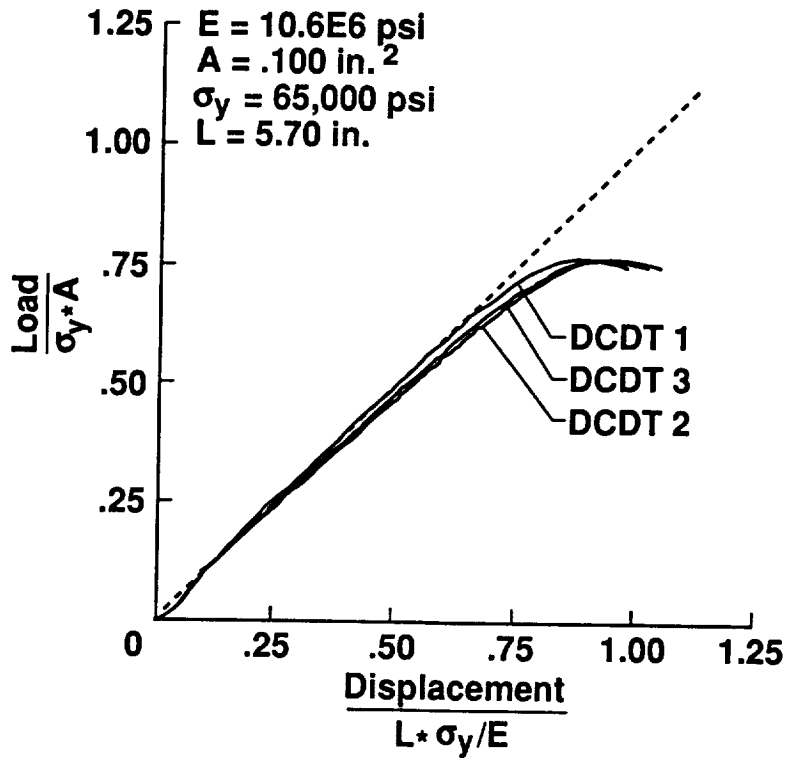
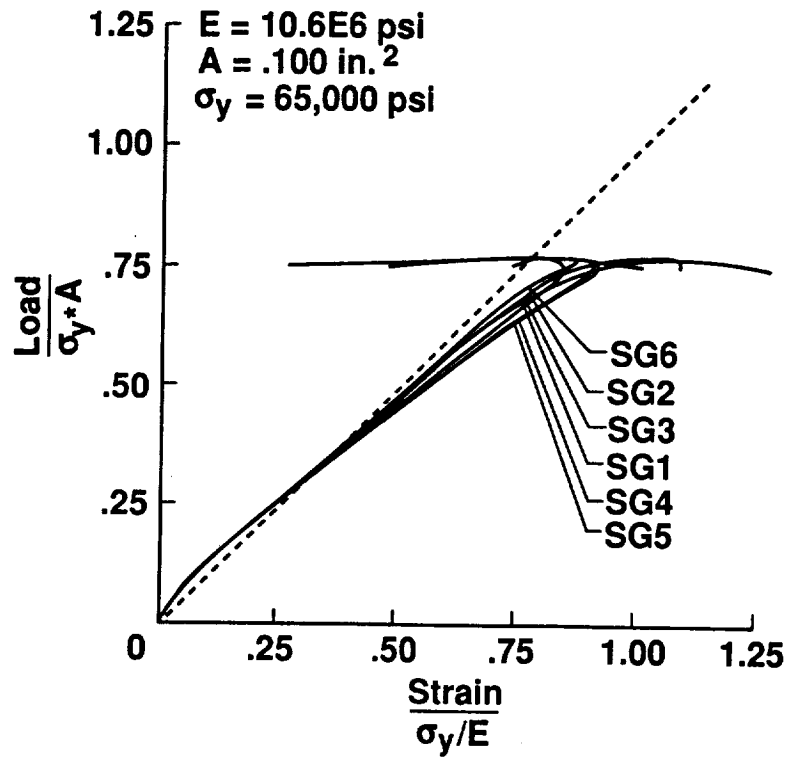


Figure 15-Strains for specimen 5

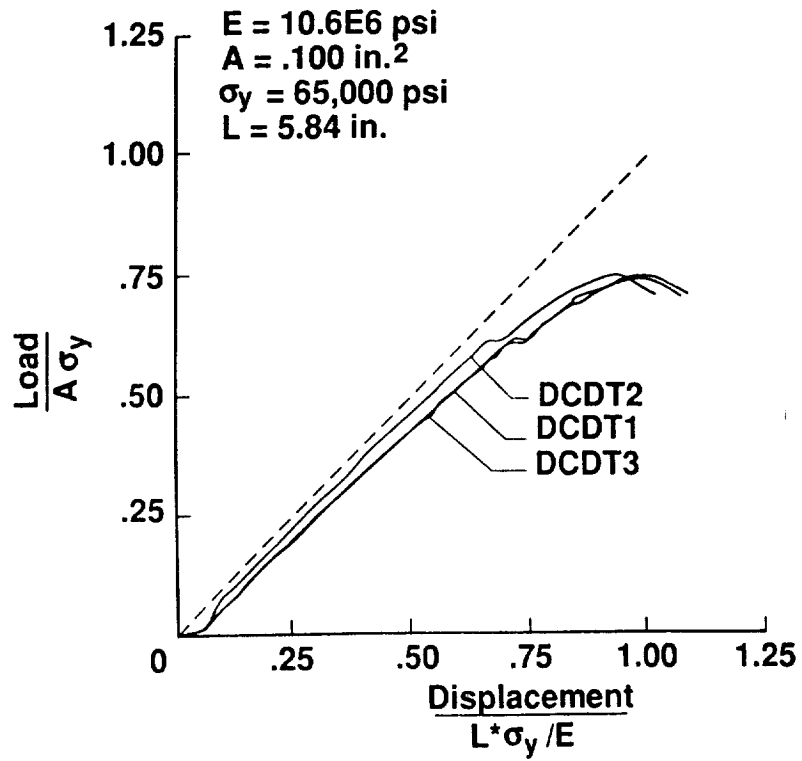
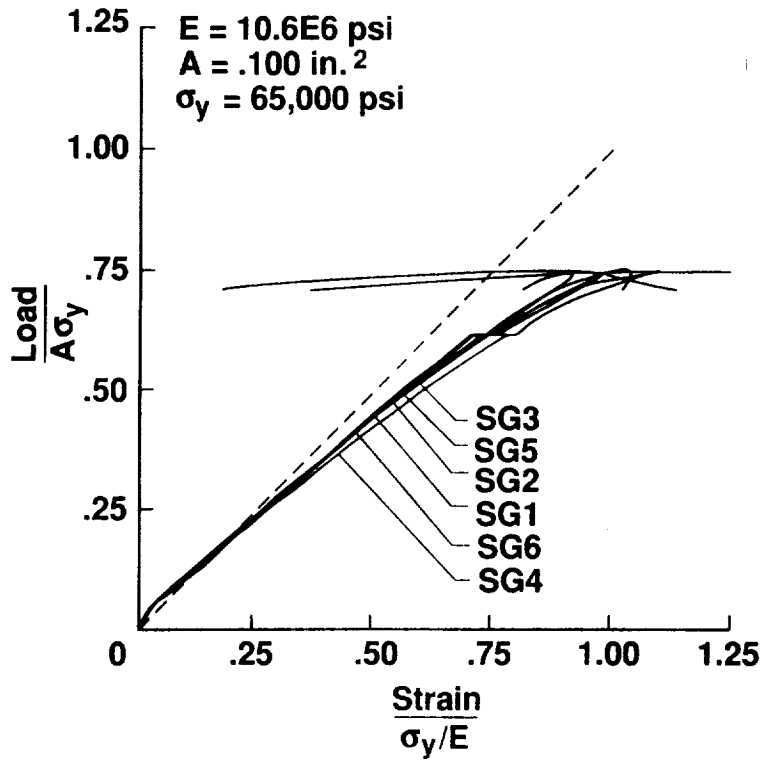


Figure 16-Strains for specimen 6

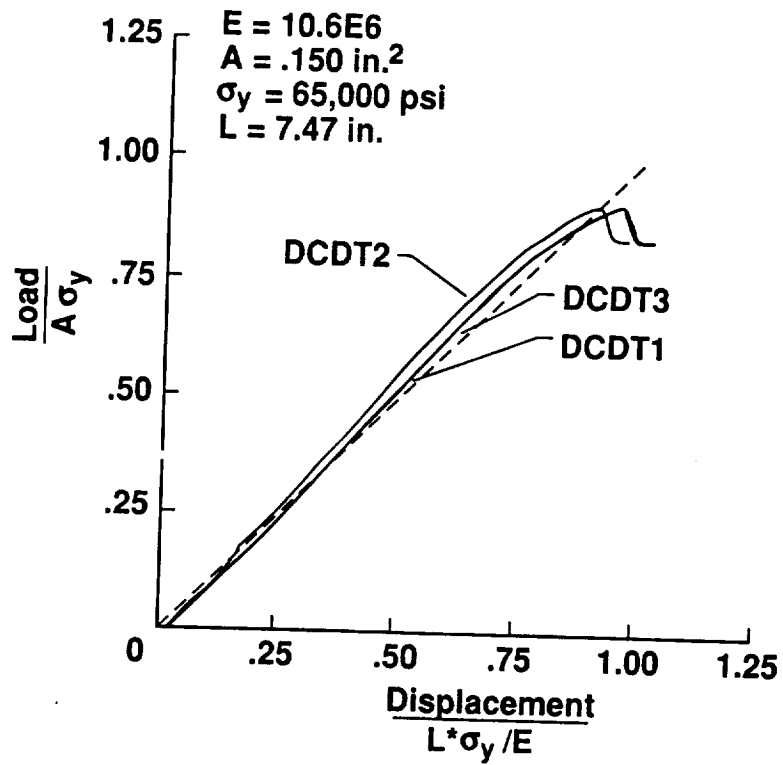
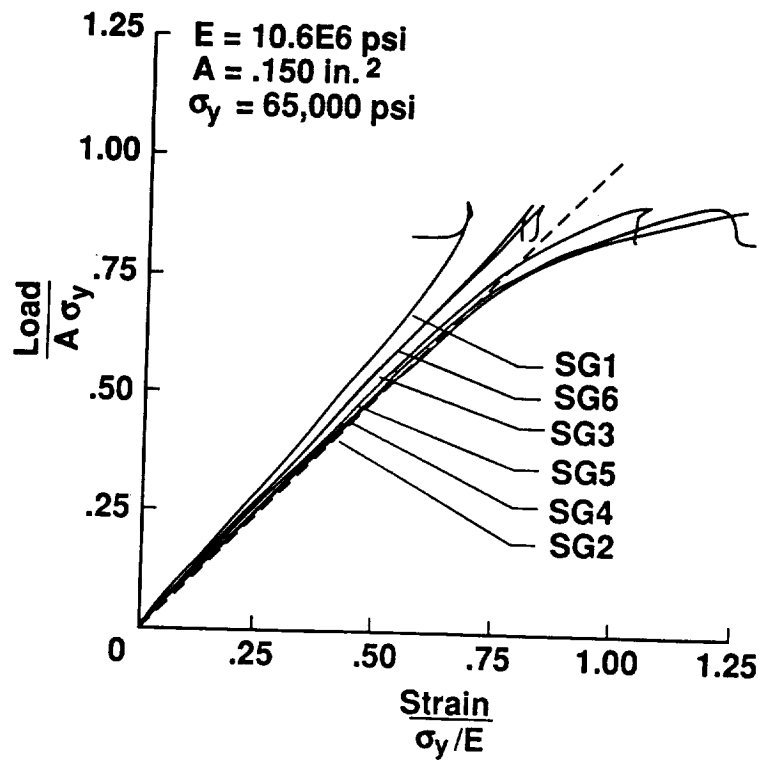


Figure 17-Strains for specimen 7

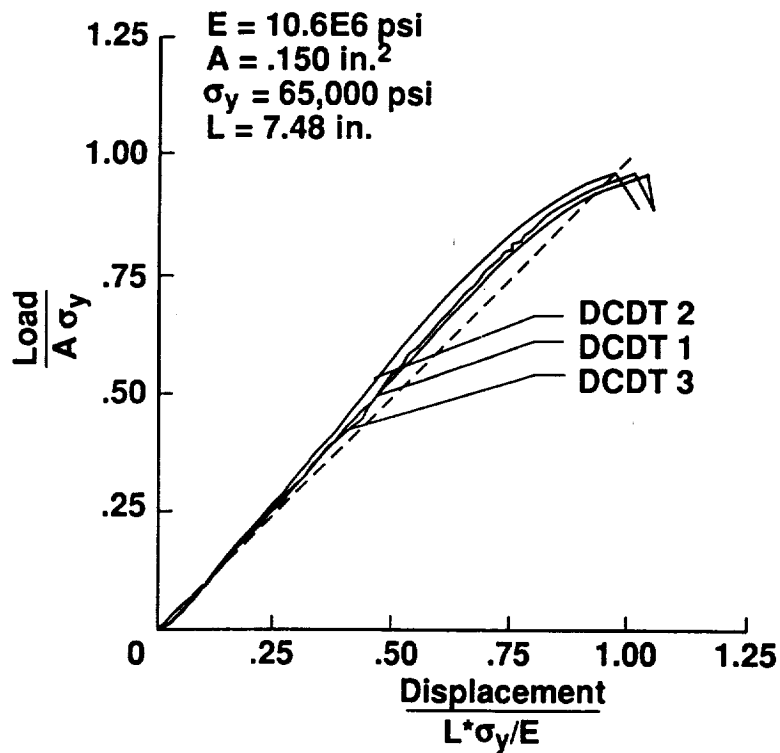
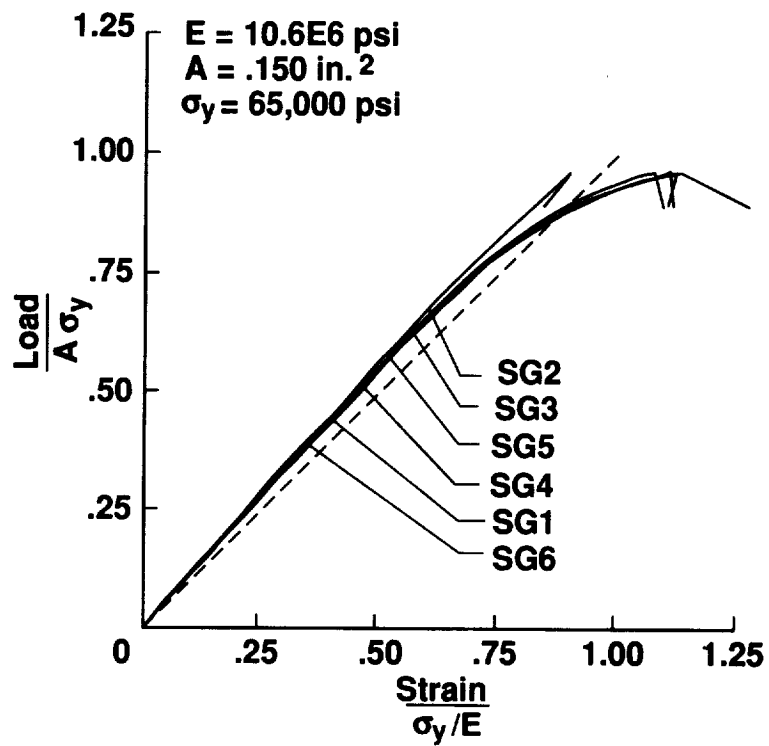


Figure 18-Strains for specimen 8

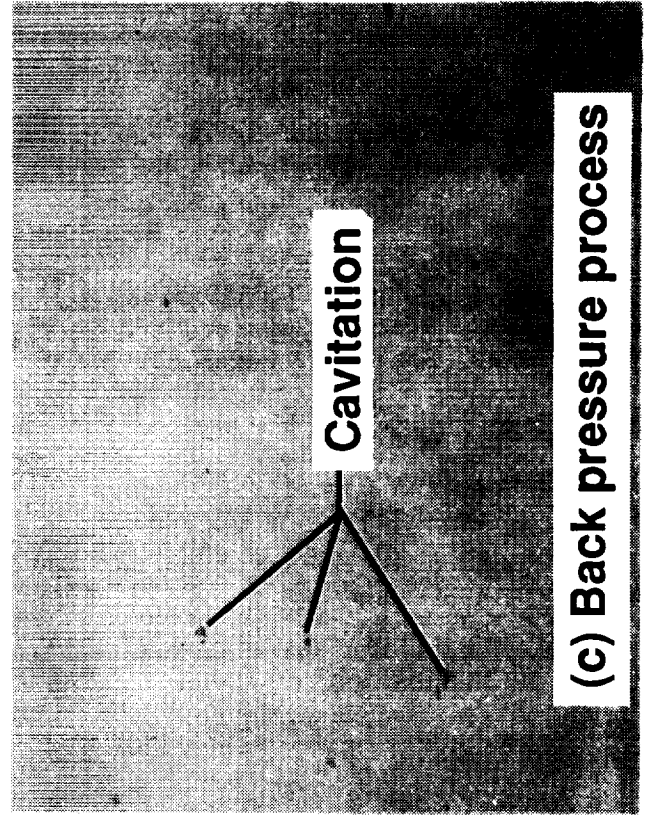
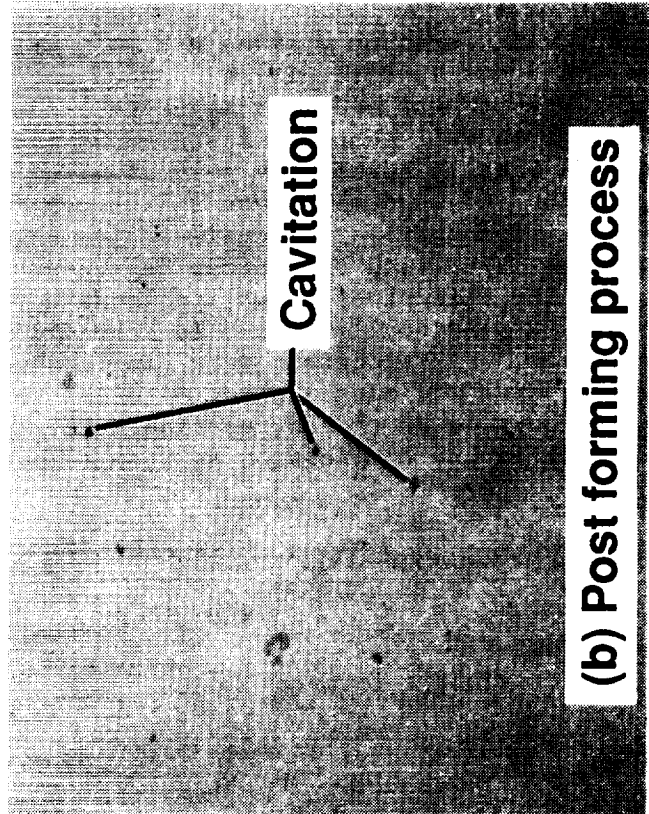
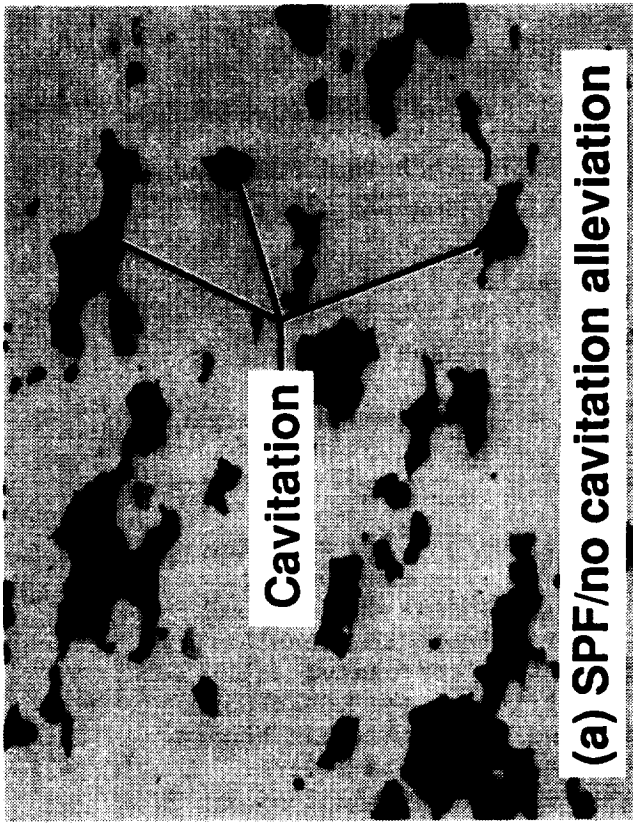


Figure 19 - Microstructure of superplastically formed 7475 aluminum alloy showing extent of cavitation (All three photos are at 400 x magnification)

ORIGINAL PAGE IS
OF POOR QUALITY



Report Documentation Page

| | | | | | |
|--|--|--|---|----------------------------|------------------|
| 1. Report No. NASA TM-104119 | | 2. Government Accession No. | | 3. Recipient's Catalog No. | |
| 4. Title and Subtitle Test of Superplastically Formed Corrugated Aluminum Compression Specimens With Beaded Webs | | | 5. Report Date June 1991 | | |
| | | | 6. Performing Organization Code | | |
| 7. Author(s) Randall C. Davis, Dick M. Royster, Thomas T. Bales, William F. James, Joseph M. Shinn, Jr. | | | 8. Performing Organization Report No. | | |
| | | | 10. Work Unit No. 510-02-13-01 | | |
| 9. Performing Organization Name and Address NASA Langley Research Center Hampton, VA 23665-5225 | | | 11. Contract or Grant No. | | |
| | | | 13. Type of Report and Period Covered Technical Memorandum | | |
| 12. Sponsoring Agency Name and Address National Aeronautics and Space Administration Washington, DC 20546-0001 | | | 14. Sponsoring Agency Code | | |
| | | | 15. Supplementary Notes Randall C. Davis, Dick M. Royster, Thomas T. Bales, and Joseph M. Shinn, Jr.: Langley Research Center, Hampton, Virginia William F. James: Lockheed Engineering and Science Company, Hampton, Virginia | | |
| 16. Abstract Corrugated wall sections provide a highly efficient structure for carrying compressive loads in aircraft and spacecraft fuselages. The superplastic forming (SPF) process offers a means to produce complex shells and panels with corrugated wall shapes. A study was made to investigate the feasibility of superplastically forming 7475-T6 aluminum sheet into a corrugated wall configuration and to demonstrate the structural integrity of the construction by testing. The corrugated configuration selected for this study has beaded web segments separating curved-cap segments. Eight test specimens were fabricated for this study. Two specimens were simply a single sheet of aluminum superplastically formed to a beaded-web, curved-cap corrugation configuration. Six specimens were single-sheet corrugations modified by adhesive bonding additional sheet material to selectively reinforce the curved-cap portion of the corrugation. The specimens were tested to failure by crippling in end compression at room temperature. | | | | | |
| 17. Key Words (Suggested by Author(s)) Corrugation Panels Test compression Aluminum superplastic forming Beaded web | | | 18. Distribution Statement Unclassified--Unlimited Subject Category 26 | | |
| 19. Security Classif. (of this report) Unclassified | | 20. Security Classif. (of this page) Unclassified | | 21. No. of pages 32 | 22. Price A03 |